

# Integrated Sensing and Communication in Distributed Antenna Networks

D. Xu, A. Khalili, X. Yu, D. W. K. Ng, and R. Schober

## Abstract

In this paper, we investigate the resource allocation design for integrated sensing and communication (ISAC) in distributed antenna networks (DANs). In particular, coordinated by a central processor (CP), a set of remote radio heads (RRHs) provide communication services to multiple users and sense several target locations within an ISAC frame. To avoid the severe interference between the information transmission and the radar echo, we propose to divide the ISAC frame into a communication phase and a sensing phase. During the communication phase, the data signal is generated at the CP and then conveyed to the RRHs via fronthaul links. As for the sensing phase, based on pre-determined RRH-target pairings, each RRH senses a dedicated target location with a synthesized highly-directional beam and then transfers the samples of the received echo to the CP via its fronthaul link for further processing of the sensing information. Taking into account the limited fronthaul capacity and the quality-of-service requirements of both communication and sensing, we jointly optimize the durations of the two phases, the information beamforming, and the covariance matrix of the sensing signal for minimization of the total energy consumption over a given finite time horizon. To solve the formulated non-convex design problem, we develop a low-complexity alternating optimization algorithm which converges to a suboptimal solution. Simulation results show that the proposed scheme achieves significant energy savings compared to two baseline schemes. Moreover, our results reveal that for efficient ISAC in wireless networks, energy-focused short-duration pulses are favorable for sensing while low-power long-duration signals are preferable for communication.

D. Xu, A. Khalili, and R. Schober are with the Institute for Digital Communications, Friedrich-Alexander-University Erlangen-Nürnberg (FAU), Germany (email: {dongfang.xu, ata.khalili, robert.schober}@fau.de). X. Yu is with Department of Electronic and Computer Engineering, the Hong Kong University of Science and Technology, Hong Kong (e-mail: eexyu@ust.hk). D. W. K. Ng is with the School of Electrical Engineering and Telecommunications, the University of New South Wales, Australia (email: w.k.ng@unsw.edu.au).

## I. INTRODUCTION

Recently, integrated sensing and communication (ISAC) has emerged as a promising technique to not only provide high data rate services to conventional communication users, but also to support various environment-aware Internet-of-Things (IoT) applications [1]. In particular, enabled by dual-functional radar-communication (DFRC) base stations (BSs), ISAC empowers radar systems and wireless communication systems to share the scarce spectrum and expensive hardware. Motivated by these advantages, various works in the literature have proposed advanced ISAC techniques to improve the performance of wireless communication systems and provide on-demand sensing services. For instance, the authors of [2] developed an efficient beamforming policy for synthesizing desired radar beam pattern in a multiuser ISAC system. Also, in [3], the authors investigated the joint design of information and sensing beamforming to maximize ISAC performance in a single-user communication system in the presence of multiple targets. However, due to the severe signal attenuation experienced by radar echoes, the potential of ISAC cannot be fully unleashed by the conventional co-located-antenna networks considered in [2], [3]. In practice, the sensing quality and the maximum sensing range of radar systems are determined by the power level of the received radar echo [4]. Yet, due to the round-trip attenuation of the echo signal, ISAC systems employing co-located antennas have to allocate a significant portion of their limited power supply to compensate for the severe path loss. For instance, a sensing target located at a distance of 200 meters from the transmitter causes a free-space round-trip path loss of roughly 170 dB for a 2.4 GHz sensing signal. Assuming an ISAC system with 5 MHz bandwidth, to ensure the echo can be distinguished from the noise having a typical power spectral density of  $-174$  dBm/Hz, the sensing signal transmit power has to be on the order of several kilowatt [4]. This results in an unaffordably high energy requirement, especially for the conventional cellular BSs considered in [2], [3], for which the power budget is usually less than 100 watts. This creates a bottleneck for achieving high-quality ISAC.

A promising approach to overcome this challenge are distributed antenna networks (DANs). Specifically, a DAN comprises a central processor (CP) and a group of low-cost remote radio heads (RRHs), where the RRHs are distributed across the network and exchange data with the CP through dedicated fronthaul links [5]. In fact, this distributed network architecture allows shortening the distance between the DFRC transmitters and the sensing targets, which is beneficial for reducing the required transmit power and extending the maximum sensing range.

Therefore, compared to conventional co-located-antenna networks, DANs are more suitable for the realization of practical ISAC systems [1]. Yet, in DANs, the information data for the communication users and the received echo of the target required for sensing information extraction have to be exchanged via fronthaul links between the RRHs and the CP. In practice, the capacity of the fronthaul links is limited due to the finite bandwidth available [6]. Hence, the capacity limitation of the fronthaul links has to be carefully considered for system design to fully unleash the potential of DAN-based ISAC. On the other hand, most existing works on ISAC design, e.g., [2], [3], propose to transmit the information signal and the sensing signal simultaneously via a mono-static radar-based BS. Yet, [2], [3] only focus on joint information beamforming and sensing beam design and do not consider the radar echo reception, which may not ensure reliable echo signal detection for practical ISAC systems. In particular, in [2], [3], the desired radar echo arrives at the BS before the information transmission ends, which causes severe self-interference (SI) at the BS. However, the SI cancellation techniques designed for conventional FD communication systems may not be able effectively suppress the SI to below the target echo power since the echo signal is severely attenuated by the round-trip path loss. To overcome this difficulty, in this paper, we propose to perform sensing and communication in orthogonal time slots and adopt pulse radar to be able to flexibly adjust the sensing range. In particular, according to pulse radar theory, the sensing range depends on the durations of the sensing pulse and the received echo [4]. As a result, the system designer has to carefully divide the available sensing time into two parts to ensure reliable echo detection at the transmitter. Although employing a DAN architecture to further enhance the performance of ISAC systems seems promising, the corresponding resource allocation design needed to facilitate high-quality sensing and communication with limited fronthaul capacity remains an open problem.

Motivated by the above observations, in this paper, we propose to achieve efficient ISAC by deploying a DAN and investigate the corresponding resource allocation algorithm design. To avoid interference between information transmission and the radar echo, we adopt an ISAC frame structure comprising two phases, i.e., a communication phase and a sensing phase. Specifically, we jointly design the durations of both phases, the beamforming vectors, and the covariance matrix of the sensing signal for minimization of the total energy consumption within an ISAC frame. The corresponding resource allocation algorithm design is formulated as a non-convex optimization problem taking into account the limited fronthaul capacity and the quality-of-service (QoS) requirements of both communication and sensing. Furthermore, we propose a

low-complexity alternating optimization (AO)-based iterative algorithm which is guaranteed to converge to a high-quality solution of the considered optimization problem.

*Notation:* Vectors and matrices are denoted by boldface lower case and boldface capital letters, respectively.  $\mathbb{R}^{N \times M}$  and  $\mathbb{C}^{N \times M}$  denote the space of  $N \times M$  real-valued and complex-valued matrices, respectively.  $|\cdot|$  and  $\|\cdot\|_2$  denote the absolute value and the  $l_2$ -norm of their arguments, respectively.  $\|\cdot\|_0$  is the  $l_0$ -norm of a vector counting the number of non-zero entries in the vector;  $(\cdot)^T$  and  $(\cdot)^H$  stand for the transpose and the conjugate transpose of their arguments, respectively.  $\mathbf{I}_N$  refers to the identity matrix of dimension  $N$ .  $\mathbb{H}^N$  denotes the set of complex Hermitian matrices of dimension  $N$ .  $\text{Tr}(\cdot)$  and  $\text{Rank}(\cdot)$  refer to the trace and rank of their arguments, respectively.  $\mathbf{A} \geq \mathbf{0}$  indicates that  $\mathbf{A}$  is a positive semidefinite matrix.  $\text{diag}(\mathbf{a})$  represents a diagonal matrix whose main diagonal elements are given by vector  $\mathbf{a}$ ;  $\mathcal{CN}(0, \sigma^2)$  specifies the distribution of a circularly symmetric complex Gaussian (CSCG) random variable with mean 0 and variance  $\sigma^2$ .  $\triangleq$  and  $\sim$  stand for “defined as” and “distributed as”, respectively.  $\mathcal{E}\{\cdot\}$  denotes statistical expectation.

## II. SYSTEM MODEL

In this section, we first introduce the proposed distributed antenna ISAC system and then present the corresponding signal and fronthaul models.

### A. DAN-Based ISAC System Model

We consider a DAN-based ISAC system which comprises a CP,  $J$  RRHs, and  $K$  users which are single-antenna devices, cf. Fig. 1. Each RRH is equipped with a uniform linear array with  $N_T$  antenna elements and is connected with the CP via an individual fronthaul link. Also, we assume that there are  $L$  desired sensing locations in the ISAC system, at each of which one potential target may exist. Moreover, as the core unit of the network, the CP is expected to perform all computations needed for operating the ISAC system. We note that when employing simultaneous information signal and sensing signal transmission, the desired radar echo usually arrives at the BS before the information transmission ends. In this case, the ISAC transmit signal may cause severe SI to the received echo signal at the BS, which is challenging to mitigate with conventional SI cancellation techniques. To overcome this difficulty, we propose to divide each ISAC frame into two phases, i.e., a communication phase and a sensing phase, having durations  $(1 - \eta)T$  and  $\eta T$ , respectively, where  $0 < \eta < 1$  denotes the time allocation variable. In

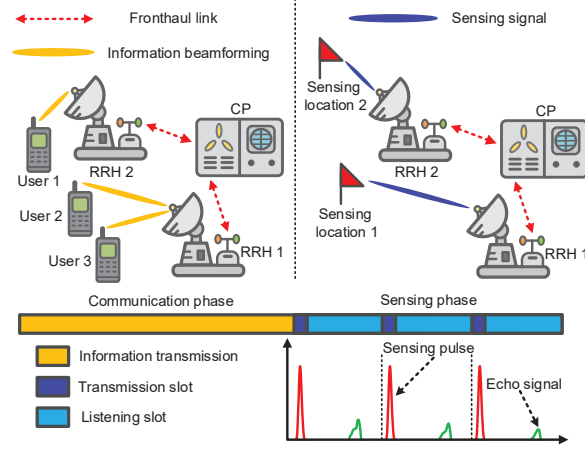


Fig. 1. Illustration of a DAN-based multiuser ISAC system comprising a CP,  $J = 2$  RRHs,  $K = 3$  users, and  $L = 2$  desired sensing locations. The CP and the RRHs exchange the information data and the samples of the received echo via fronthaul links. The color bar indicates the proposed frame structure comprising a communication phase and a sensing phase. In the communication phase, the RRHs jointly implement beamforming to serve all the users in a collaborative manner. Also, the sensing phase is divided into  $M = 3$  rounds, where each round contains a transmission slot for pulse emission and a listening slot for echo reception. The red and green signals in the bottom-right figure represent the sensing pulse and echo signal, respectively.

particular, in the communication phase, the CP computes the beamforming vectors for the users, and forwards the information data of the users and the control signals for resource allocation to the RRHs via the fronthaul links.<sup>1</sup> On the other hand, we propose to assign a dedicated RRH to each sensing location to facilitate high-quality sensing based on an energy-focused beam. Assuming  $J \geq L$ , the RRH assignment policy is pre-designed in an offline manner<sup>2</sup> and is utilized for the online resource allocation optimization, which facilitates a low-complexity ISAC design. Hence, there are  $L$  pre-determined RRH-target pairs in the considered system. During the sensing phase, the CP computes the covariance matrix of the sensing signal for each pre-designed RRH-target pair and forwards the resulting resource allocation policy to each RRH via a fronthaul link. Then, all RRH concurrently emit highly-directional beams towards their respective paired target locations in the transmission slot of duration of  $t_p$  before switching to the listening mode to receive the echoes. To facilitate high-quality sensing, the sensing phase is

<sup>1</sup>In practice, the fronthaul links can be established via out-of-band radio frequency links or free-space optical links [6].

<sup>2</sup>In practice, the RRH assignment policy can be based on the system geometry and the sensing application scenario, e.g., by pairing RRHs and sensing locations based on distance.

divided into  $M$  sensing slots [4], each of which has a duration of  $\frac{\eta T}{M}$ . The received echoes are transferred to the CP via the fronthaul link to facilitate the acquisition of fine-resolution sensing information. Besides, to investigate the performance upper bound of the considered system, we assume perfect channel state information of the users and the desired target locations is available at the CP. For notational simplicity, we collect the indices of the RRHs, users, and desired target locations in sets  $\mathcal{J} = \{1, \dots, J\}$ ,  $\mathcal{K} = \{1, \dots, K\}$ , and  $\mathcal{L} = \{1, \dots, L\}$ , respectively.

*Remark 1:* We note that the proposed RRH-target pairing policy facilitates power-efficient high-quality sensing in the considered DAN-based ISAC system. In particular, this policy simplifies the sensing beam design, i.e., it facilitates the use of highly-directional beam patterns, which helps avoid severe clutter and interference between different RRH-target pairs [4]. Also, the proposed policy allows us to sense each target location via the nearest RRH, which potentially improves the network power efficiency. As an alternative strategy, all the  $J$  RRHs may concurrently sense all target locations. However, this would result in a complicated multi-beam pattern synthesis problem and may lead to severe crosstalk between different RRHs, which would degrade sensing quality.

### B. Signal Model

In the communication phase,  $K$  independent data streams are transmitted simultaneously to the  $K$  users. In particular, a beamforming vector dedicated to user  $k$ ,  $\mathbf{w}_{j,k} \in \mathbb{C}^{N_T \times 1}$ , is generated at the CP and is conveyed to RRH  $j$  via fronthaul link  $j$ . For ease of presentation, we define a super-vector  $\mathbf{w}_k = [(\mathbf{w}_{1,k})^T, (\mathbf{w}_{2,k})^T, \dots, (\mathbf{w}_{J,k})^T]^T \in \mathbb{C}^{N_T J \times 1}$  to collect all the beamforming vectors for serving user  $k$ . The transmit signal vector at the RRHs is given by  $\sum_{k \in \mathcal{K}} \mathbf{w}_k b_k$ , where  $b_k \in \mathbb{C}$  denotes the information-bearing symbol intended for user  $k$  and we assume  $\mathcal{E}\{|b_k|^2\} = 1$ ,  $\forall k \in \mathcal{K}$ , without loss of generality. The received signal at user  $k$  is given by

$$y_{U_k} = \mathbf{h}_k^H \mathbf{w}_k b_k + \mathbf{h}_k^H \sum_{r \in \mathcal{K} \setminus \{k\}} \mathbf{w}_r b_r + n_{U_k}. \quad (1)$$

Here, vector  $\mathbf{h}_k \in \mathbb{C}^{N_T J \times 1}$  represents the channel between the  $J$  RRHs and user  $k$ .  $n_{U_k} \sim \mathcal{CN}(0, \sigma_{U_k}^2)$  denotes the equivalent additive white Gaussian noise (AWGN) at user  $k$  with variance  $\sigma_{U_k}^2$ .

In the sensing phase, for the  $l$ -th RRH-target pair, a sensing signal  $\mathbf{s}_l \in \mathbb{C}^{N_T \times 1}$  is transmitted by the RRH to illuminate the desired target location. In this paper, we assume the same sensing signal  $\mathbf{s}_l$  is transmitted in each of the  $M$  sensing rounds and model  $\mathbf{s}_l$  as a CSCG random vector

with zero mean and covariance matrix  $\mathbf{S}_l \geq \mathbf{0}$  [3]. We note that  $\mathbf{s}_l$  is generated locally at the associated RRH based on the optimized resource allocation policy, i.e., the fronthaul links are not involved. The received signal at the  $l$ -th RRH is modeled as [7]

$$\mathbf{y}_l = \underbrace{\mathbf{g}_{l,l}\mathbf{g}_{l,l}^H\mathbf{s}_l}_{\text{Desired echo}} + \underbrace{\sum_{q \in \mathcal{L} \setminus \{l\}} \left( \sum_{p \in \mathcal{L}} \mathbf{g}_{l,p}\mathbf{g}_{q,p}^H\mathbf{s}_q + \mathbf{g}_{l,q}\mathbf{g}_{l,q}^H\mathbf{s}_l \right)}_{\text{Clutter}} + \mathbf{n}_l, \quad (2)$$

where  $\mathbf{n}_l \sim \mathcal{CN}(\mathbf{0}, \sigma_l^2 \mathbf{I}_{N_T})$  denotes the AWGN at RRH  $l$  with noise variance  $\sigma_l^2$ . Moreover, similar to [2], in this paper, we assume pure line-of-sight (LoS) channels between the desired sensing locations and the RRHs. In particular, the channel between RRH  $q$  and location  $l$  is denoted by vector  $\mathbf{g}_{q,l} \in \mathbb{C}^{N_T \times 1}$ ,  $\forall q, l \in \mathcal{L}$ , and is given by

$$\mathbf{g}_{q,l} = \sqrt{\beta_{q,l}} \mathbf{a}(\phi_{q,l}), \quad (3)$$

where  $\beta_{q,l} \in \mathbb{R}$  and  $\mathbf{a}(\phi_{q,l}) \in \mathbb{C}^{N_T \times 1}$  denote the channel gain and the steering vector between RRH  $q$  and location  $l$ , respectively. In particular,  $\beta_{q,l}$  is given by  $\beta_{q,l} = \gamma_l \frac{\varrho_0}{d_{q,l}^2}$ , where  $d_{q,l}$  is the distance between RRH  $q$  and location  $l$  and  $\gamma_l \in \mathbb{R}$  is the radar cross-section of target  $l$  [7]. The value of constant  $\varrho_0 = (\frac{c}{4\pi f_c})^2$  depends on the system center frequency  $f_c$  and the speed of light  $c$ . Moreover, vector  $\mathbf{a}(\phi_{q,l})$  is given by  $\mathbf{a}(\phi_{q,l}) = \left[ 1, e^{j2\pi\omega \sin\phi_{q,l}}, \dots, e^{j2\pi\omega(N_T-1)\sin\phi_{q,l}} \right]^T$  with  $\phi_{q,l}$  and  $\omega$  being the angle of departure (AoD) from RRH  $q$  to location  $l$  and the normalized spacing between adjacent antenna elements [2], respectively. To facilitate the presentation, we define matrix  $\mathbf{G}_{l,p,q} \in \mathbb{C}^{N_T \times N_T}$  to characterize the channel of the two-hop link from RRH  $q$  to RRH  $l$  via target location  $p$ , where  $\mathbf{G}_{l,p,q} = \mathbf{g}_{l,p}\mathbf{g}_{q,p}^H$ ,  $\forall l, p, q \in \mathcal{L}$  [7].

### C. Fronthaul Model

Via the fronthaul links, the information data of all users and the samples of the received echoes are exchanged between the RRHs and the CP in the communication and sensing phases, respectively. Specifically, in the communication phase, we model the required fronthaul capacity<sup>3</sup> for RRH  $j$  as follows [6]

$$C_j^C = \frac{\sum_{k \in \mathcal{K}} \|\mathbf{w}_{j,k}\|_2 N_k^C}{(1 - \eta)TW_F} \quad (\text{bits/s/Hz}), \quad j \in \mathcal{J}. \quad (4)$$

<sup>3</sup>In this paper, we assume that for each fronthaul link, a fixed amount of fronthaul capacity has already been reserved for forwarding the resulting resource allocation policy from the CP to the RRHs. Thus, this part is not considered in (4).

Here, constants  $N_k^C$  and  $W_F$  denote the number of bits dedicated to user  $k$  during one ISAC frame and the bandwidth of the fronthaul links, respectively. To facilitate the presentation, we define  $\bar{R}_{\text{req}_k} = \frac{N_k^C}{TW_F}$  (bits/s/Hz) as the required data rate for delivering the data intended for user  $k$  via a fronthaul link to an RRH. Moreover, the value of  $\sum_{k \in \mathcal{K}} \|\mathbf{w}_{j,k}\|_2$  belongs to set  $\mathcal{K}$  and represents the number of users served by RRH  $j$ . In practice, due to the limited capacity of the fronthaul links, each RRH may not be able to simultaneously serve all  $K$  users. Instead, based on the resource allocation policy, the CP can facilitate partial cooperation, i.e., delivering the information data dedicated to user  $k$  only to a subset of the RRHs. This can be achieved by setting  $\mathbf{w}_{i,k} = \mathbf{0}$ ,  $i \in \mathcal{J}$ , which excludes RRH  $i$  from participating in the joint information transmission to user  $k$ . On the other hand, for target sensing, the RRH emits beams of duration  $t_p$  and then switches to the listening mode to receive the corresponding echoes until the end of the sensing round. According to pulse radar theory [4], the minimum sensing range and the maximum sensing range of the considered ISAC system are given by

$$R_{\min} = \frac{ct_p}{2} \quad \text{and} \quad R_{\max} = \frac{c(\frac{\eta T}{M} - t_p)}{2}, \quad (5)$$

respectively. In particular,  $R_{\min}$  and  $R_{\max}$  denote the minimum and maximum distances that a radar with pulse duration  $t_p$  and subsequent reception duration  $(\frac{\eta T}{M} - t_p)$  can detect, respectively. We note that unlike in the communication phase, where the RRHs receive only data symbols from the CP, in the sensing phase, the RRH has to first sample and quantize the received echo based on the desired sensing resolution, and then forward the quantized data to the CP [8]. Based on the above considerations, for each sensing round of duration  $(\frac{\eta T}{M} - t_p)$ , we model the required fronthaul capacity for conveying the sampled and quantized echoes from a RRH to the CP as follows [9]

$$C^S = \frac{(R_{\max} - R_{\min})N_b}{\Delta R(\frac{\eta T}{M} - t_p)W_F} \quad (\text{bits/s/Hz}). \quad (6)$$

Here, parameter  $\Delta R > 0$  denotes the pre-defined target resolution of the radar in meter and measures the ability of a radar to distinguish between the desired target and other objects in the vicinity.<sup>4</sup> Besides, constant  $N_b$  denotes the number of bits required for quantizing the echo without causing saturation.

<sup>4</sup>In practice, the value of  $\Delta R$  is determined by the width of the pulse, type of target, and efficiency of the radar [4].



### III. PROBLEM FORMULATION

In this section, we formulate the resource allocation algorithm design as a non-convex optimization problem, after defining the adopted QoS metrics for the considered ISAC system.

#### A. Performance Metrics

During the communication phase, the achievable rate (bits/s/Hz) of user  $k$  is given by

$$R_k = \log_2 \left( 1 + \frac{|\mathbf{h}_k^H \mathbf{w}_k|^2}{\sum_{r \in \mathcal{K} \setminus \{k\}} |\mathbf{h}_k^H \mathbf{w}_r|^2 + \sigma_{U_k}^2} \right). \quad (7)$$

On the other hand, to facilitate high-quality sensing during the sensing phase, the desired sensing location has to be illuminated by an energy-focusing beam with low side lobe leakage such that the desired echoes can be easily distinguished from clutter. To this end, we discretize the angular domain  $[0, 2\pi]$  into  $I$  directions and generate the ideal beam pattern  $\{P(\theta_i)\}_{i=1}^I$  offline, where  $P(\theta_i)$  denotes the beam pattern power in direction  $\theta_i$ . Specifically, for the  $l$ -th RRH-target pair,  $\{P_l(\theta_i)\}_{i=1}^I$  is given by

$$P_l(\theta_i) = \begin{cases} 1, & |\theta_i - \phi_{l,l}| \leq \frac{\psi_l}{2}, \\ 0, & \text{otherwise} \end{cases}, \quad \forall l \in \mathcal{L}, \quad (8)$$

where  $\psi_l$  is the desired beamwidth of the ideal beam pattern for the  $l$ -th RRH-target pair. Since the ideal beam pattern is difficult to generate in practice, we approximate it by suitably choosing the covariance matrix of the sensing signal [8], i.e.,  $\mathbf{S}_l$ . To quantify the beam pattern matching accuracy, in this paper, we adopt the difference between the ideal beam pattern and the actual beam pattern as a performance metric for sensing as follows

$$D_l(\mathbf{S}_l, \xi_l) = \sum_{i=1}^I |P_l(\theta_i) - \xi_l \mathbf{a}^H(\theta_i) \mathbf{S}_l \mathbf{a}(\theta_i)|, \quad \forall l \in \mathcal{L}, \quad (9)$$

where  $\xi_l$  is a scaling factor to be optimized for the  $l$ -th RRH-target pair.<sup>5</sup> Moreover, to facilitate reliable detection of the desired echo signal at the RRH, we consider two additional performance metrics for sensing. On the one hand, to ensure the desired echo signal can be effectively captured by the paired RRH, we consider the received echo power at RRH  $l$  which is given

<sup>5</sup>Different from some existing works, e.g., [3], in this paper, we propose to use  $\xi_l$  to scale the actual beam pattern instead of the ideal beam pattern. By doing so, we can flexibly control the beam pattern mismatch error to satisfy different beam synthesis accuracy requirements for a given ideal beam pattern [4].

by  $\text{Tr}(\mathbf{G}_{l,l,l}\mathbf{S}_l\mathbf{G}_{l,l,l}^H)$ . On the other hand, to effectively suppress the clutter, we consider the interference at RRH  $l$ , i.e.,  $I_l$ , which is given by

$$I_l = \sum_{q \in \mathcal{L} \setminus \{l\}} \left( \sum_{p \in \mathcal{L}, p' \in \mathcal{L}} \text{Tr}(\mathbf{G}_{l,p,q}\mathbf{S}_q\mathbf{G}_{l,p',q}^H) + \sum_{q' \in \mathcal{L}} \text{Tr}(\mathbf{G}_{l,q,l}\mathbf{S}_l\mathbf{G}_{l,q',l}^H) + \text{Tr}(\mathbf{G}_{l,l,l}\mathbf{S}_l\mathbf{G}_{l,q,l}^H) \right). \quad (10)$$

### B. Optimization Problem Formulation

In this paper, our objective is to minimize the total energy consumption of the considered system over a given time horizon of duration  $T$  and for a pre-designed RRH-target assignment policy. In particular, given the ideal beam pattern gain  $\{P_l(\theta_i)\}_{i=1}^M$ , then the desired time allocation variable  $\eta$ , the sensing beam duration  $t_p$ , the beamforming vectors  $\mathbf{w}_k$ , and the sensing beam pattern  $\mathbf{S}_l$  can be obtained by solving the following problem

$$\begin{aligned} & \underset{\mathbf{S}_l \in \mathbb{H}^{N_T}, \mathbf{w}_k, \eta, t_p, \xi_l > 0}{\text{minimize}} & f & \triangleq (1 - \eta)T \sum_{k \in \mathcal{K}} \|\mathbf{w}_k\|_2^2 + Mt_p \sum_{l \in \mathcal{L}} \text{Tr}(\mathbf{S}_l) \\ & \text{s.t. C1: } R_k & \geq \frac{\bar{R}_{\text{req}_k}}{(1 - \eta)}, \quad \forall k, & \text{C2: } \text{Tr}(\mathbf{G}_l \mathbf{S}_l \mathbf{G}_l^H) & \geq P_{\text{req}_l}, \quad \forall l, \\ & \text{C3: } I_l & \leq P_{\text{tol}_l}, \quad \forall l, & \text{C4: } D_l(\mathbf{S}_l, \xi_l) & \leq \varepsilon_l, \quad \forall l, \\ & \text{C5: } \sum_{k \in \mathcal{K}} \|\mathbf{w}_{j,k}\|_2^2 & \leq P_{T_j}^{\max}, \quad \forall j, & \text{C6: } \text{Tr}(\mathbf{S}_l) & \leq P_{T_l}^{\max}, \quad \forall l, \\ & \text{C7: } \mathbf{S}_l \geq \mathbf{0}, \quad \forall l, & \text{C8: } \frac{\sum_{k \in \mathcal{K}} \|\|\mathbf{w}_{j,k}\|_2\|_0 \bar{R}_{\text{req}_k}}{1 - \eta} & \leq C_{F_j}^{\max}, \quad \forall j, \\ & \text{C9: } \frac{(R_{\max} - R_{\min})N_b}{\Delta R(\frac{\eta T}{M} - t_p)W_F} & \leq C_{F_l}^{\max}, \quad \forall l, & \text{C10: } \frac{c(\frac{\eta T}{M} - t_p)}{2} & \geq d_{l,l} \geq \frac{ct_p}{2}, \quad \forall l, \\ & \text{C11: } t_{\min} & \leq t_p, & \text{C12: } 0 < \eta < 1. & \end{aligned} \quad (11)$$

In constraint C1, we impose a lower bound on the achievable rate of user  $k$ , i.e.,  $\bar{R}_{\text{req}_k}$ , to guarantee satisfactory communication services within an ISAC frame. To ensure that the desired echo can be effectively detected at RRH  $l$ , we restrict the minimum echo power strength and the maximum crosstalk interference caused by all the other RRHs to  $P_{\text{req}_l}$  and  $P_{\text{tol}_l}$ , respectively, as specified in constraints C2 and C3, respectively. To generate favorable highly-directional beams, in constraint C4, we restrict the difference between the ideal beam pattern and the actual beam pattern to be below an error tolerance  $\varepsilon_l$  [10]. Constant  $P_{T_j}^{\max}$  in C5 denotes the per RRH power budget for all  $J$  RRHs during the communication phase. Similarly, during the sensing phase, we limit the maximum transmit power of the RRHs to  $P_{T_l}^{\max}$ ,  $\forall l \in \mathcal{L}$ , as shown in constraint C6.  $\mathbf{S}_l \in \mathbb{H}^{N_T}$  and constraint C7 guarantee that  $\mathbf{S}_l$  is a covariance matrix. In constraint C8, we

constrain the capacity consumption of fronthaul link  $j$  to the maximum capacity allowance  $C_{F_j}^{\max}$ . Constraint C9 is imposed to ensure that for the  $l$ -th RRH-target pair, the delivery of the echo via fronthaul link  $l$  does not violate the maximum capacity allowance  $C_{F_l}^{\max}$  in each sensing round. For each RRH-target pair, the desired target location should be included in the radar sensing range [4], as indicated in constraint C10. Also, constraint C11 specifies the minimum duration of the sensing pulse, i.e.,  $t_{\min}$ . In practice, due to the limitations of the hardware, a minimum time interval is required to switch between transmission and listening [4]. Constraint C12 indicates the range of the time allocation variable.

We note that optimization problem (11) is non-convex. Specifically, the non-convexity stems from the coupled optimization variables in the objective function, the fractional functions in constraint C1, and the non-convex  $l_0$ -norm in constraint C8. In general, it is challenging to find the globally optimal solution to problem (11) in polynomial time. To overcome this difficulty, in the next section, we develop an AO-based algorithm which can produce a high-quality solution of (11) with low computational complexity.

#### IV. SOLUTION OF THE OPTIMIZATION PROBLEM

In this section, we tackle optimization problem (11). In particular, we first recast (11) into an equivalent form and then, develop a computationally-efficient AO algorithm for handling the resulting problem.

##### A. Problem Reformulation

We start by defining the beamforming matrices  $\mathbf{W}_k = \mathbf{w}_k \mathbf{w}_k^H$ ,  $\forall k \in \mathcal{K}$ . Moreover, we introduce an auxiliary binary optimization variable  $\zeta_{j,k}$  and recast (11) in equivalent form as follows

$$\begin{aligned}
 & \underset{\mathbf{S}_l \in \mathbb{H}^{N_T}, \mathbf{W}_k \in \mathbb{H}^{N_T \times J}, \eta, t_p, \xi_l > 0, \zeta_{j,k}}{\text{minimize}} && f \\
 & \text{s.t. C1-C7, C9-C12,} \\
 & \text{C8: } \frac{\sum_{k \in \mathcal{K}} \zeta_{j,k} \bar{R}_{\text{req}_k}}{1 - \eta} \leq C_{F_j}^{\max}, \forall j, & \text{C13: } \text{Tr}(\mathbf{W}_k \mathbf{D}_j) \leq \zeta_{j,k} P_{T_j}^{\max}, \forall j, \forall k, \\
 & \text{C14: } \zeta_{j,k} \in \{0, 1\}, \forall j, \forall k, & \text{C15: } \mathbf{W}_k \geq \mathbf{0}, \forall k, \text{ C16: } \text{Rank}(\mathbf{W}_k) \leq 1, \forall k. \quad (12)
 \end{aligned}$$

Here, to facilitate the presentation, we define a block diagonal matrix  $\mathbf{D}_j \in \mathbb{R}^{N_T J \times N_T J}$  which is given by  $\mathbf{D}_j \triangleq \text{diag}(\underbrace{0, \dots, 0}_{(j-1)N_T}, \underbrace{1, \dots, 1}_{N_T}, \underbrace{0, \dots, 0}_{(J-j)N_T})$ . Moreover, constraints C13 and C14 are

two auxiliary constraints to ensure the equivalence between (11) and (12). The auxiliary binary optimization variable  $\zeta_{j,k}$  can be regarded as a binary indicator for whether the data of user  $k$  is conveyed to RRH  $j$  for information transmission or not. In particular, for  $\text{Tr}(\mathbf{W}_k \mathbf{D}_j) > 0$ , the data of user  $k$  occupies  $\frac{\bar{R}_{\text{req}_k}}{1-\eta}$  bit/s/Hz of the capacity of fronthaul link  $j$ , leading to  $\zeta_{j,k} = 1$  and vice versa. On the other hand,  $\mathbf{W}_k \in \mathbb{H}^{N_T J}$  and constraints C15 and C16 are imposed to guarantee that  $\mathbf{W}_k = \mathbf{w}_k \mathbf{w}_k^H$  holds after optimization. As (11) and (12) are equivalent, next, we focus on the optimization problem in (12) and develop a corresponding resource allocation algorithm.

### B. Handling Binary Constraint C14

The binary constraint C14 is an obstacle to efficiently tackling (12). To circumvent this obstacle, we replace constraint C14 with the following two equivalent constraints

$$\text{C14a: } 0 \leq \zeta_{j,k} \leq 1, \quad \text{C14b: } \sum_{j \in \mathcal{J}} \sum_{k \in \mathcal{K}} (\zeta_{j,k} - \zeta_{j,k}^2) \leq 0. \quad (13)$$

Here, constraint C14b is the difference of two convex functions, which makes the constraint non-convex. To address this issue, we resort to a penalty-based method [11] and rewrite the objective function in (11) as

$$\bar{f} = f + \mu \sum_{j \in \mathcal{J}} \sum_{k \in \mathcal{K}} (\zeta_{j,k} - \zeta_{j,k}^2), \quad (14)$$

where  $\mu \gg 1$  is the penalty factor penalizing the violation of constraint C14b. Then, we apply successive convex approximation to overcome the non-convexity of constraint C14b. In particular, we construct a global underestimator for the term  $\zeta_{j,k}^2$  by expanding it to a first-order Taylor series at feasible point  $\zeta_{j,k}^{(i)}$  and rewrite  $\bar{f}$  in (14) as follows

$$\bar{f} = f + \mu \sum_{j \in \mathcal{J}} \sum_{k \in \mathcal{K}} [\zeta_{j,k} - 2\zeta_{j,k}^{(i)}\zeta_{j,k} + (\zeta_{j,k}^{(i)})^2], \quad (15)$$

where superscript  $i$  indicates the iteration index of the optimization algorithm.

### C. Alternating Optimization-Based Algorithm

Next, for handling the coupled optimization variables in (12), we divide the optimization variables into two blocks, i.e.,  $\{\mathbf{S}_l, \mathbf{W}_k, \zeta_{j,k}\}$  and  $\{\eta, t_p, \xi_l, \zeta_{j,k}\}$ , and solve the resulting two subproblems in an alternating manner.

*Block 1:* We first obtain  $\{\mathbf{S}_l, \mathbf{W}_k, \zeta_{j,k}\}$  by solving the following problem

$$\begin{aligned}
& \underset{\mathbf{S}_l \in \mathbb{H}^{N_T}, \mathbf{W}_k \in \mathbb{H}^{N_T J}, \zeta_{j,k}}{\text{minimize}} && \bar{f} \\
& \text{s.t.} && \text{C1: } \text{Tr}(\mathbf{H}_k \mathbf{W}_k) \geq \chi_k \left( \sum_{r \in \mathcal{K} \setminus \{k\}} \text{Tr}(\mathbf{H}_k \mathbf{W}_r) + \sigma_{U_k}^2 \right), \forall k, \\
& && \text{C2-C8, C13, C14a, C15, C16,}
\end{aligned} \tag{16}$$

where scalar  $\chi_k$  is defined as  $\chi_k = 2^{\frac{\bar{R}_{\text{req}_k}}{1-\eta}} - 1$  for notational simplicity. By employing semidefinite relaxation (SDR), we omit the only non-convex constraint in (16), i.e., constraint C16, and solve the remaining problem by applying standard convex problem solvers such as CVX. The tightness of the SDR is revealed in the following theorem.

*Theorem 1:* The optimal beamforming matrix  $\mathbf{W}_k^*$  of the rank constraint-relaxed version of (16) is a unit-rank matrix.

*Proof:* The proof of Theorem 1 follows similar steps as the proof in [12, Appendix A], and is thus omitted here due to page limitation.

*Block 2:* For given  $\{\mathbf{S}_l, \mathbf{W}_k, \zeta_{j,k}\}$ , we obtain  $\{\eta, t_p, \xi_l, \zeta_{j,k}\}$  by solving the following convex optimization problem

$$\begin{aligned}
& \underset{\eta, t_p, \xi_l > 0, \zeta_{j,k}}{\text{minimize}} && \bar{f} \\
& \text{s.t.} && \text{C1, C4, C8-C13, C14a.}
\end{aligned} \tag{17}$$

The proposed AO-based algorithm is summarized in **Algorithm 1**. Note that the values of  $\bar{f}$  in (16) and (17) are monotonically non-increasing in each iteration of **Algorithm 1**. Moreover, according to [11] and [13], for a sufficiently large  $\mu$ , **Algorithm 1** is guaranteed to converge to a stationary value of the objective function of (11) in polynomial time, producing thus a high-quality solution for (11). The computational complexity of **Algorithm 1** is given by  $\mathcal{O}\left(\log(1/\delta)\left((KJ + 2K + J)(N_T J)^3 + (KJ + 2K + J)^2(N_T J)^2 + (KJ + 2K + J)^3 + 4L(N_T)^3 + (4L)^2(N_T)^2 + (4L)^3\right)\right)$ , where  $\mathcal{O}(\cdot)$  is the big-O notation and  $\delta$  is the convergence tolerance of **Algorithm 1**.

## V. SIMULATION RESULTS

This section provides simulation results to evaluate the performance of the proposed DAN-based ISAC design. In particular, we assume that there are  $J = 3$  RRHs connected to the CP in the considered cell, as shown in Fig. 2, and each RRH is equipped with  $N_T = 6$  antennas.

---

**Algorithm 1** AO-Based Algorithm
 

---

- 1: Set iteration index  $i = 1$ , convergence tolerance  $0 < \delta \ll 1$ , and penalty factor  $\mu \gg 1$ , initialize the optimization variables  $\mathbf{W}_k^{(i)}$ ,  $\mathbf{S}_l^{(i)}$ ,  $\eta^{(i)}$ ,  $t_p^{(i)}$ ,  $\xi_l^{(i)}$ , and  $\zeta_{j,k}^{(i)}$ .
  - 2: **repeat**
  - 3:   Solve the relaxed version of (16) for given  $\eta^{(i)}$ ,  $t_p^{(i)}$ ,  $\xi_l^{(i)}$ ,  $\zeta_{j,k}^{(i)}$ , and update the solution  $\mathbf{W}_k^{(i+1)}$ ,  $\mathbf{S}_l^{(i+1)}$ ,  $\zeta_{j,k}^{(i+1)}$
  - 4:   Solve (17) for  $\mathbf{W}_k = \mathbf{W}_k^{(i+1)}$ ,  $\mathbf{S}_l = \mathbf{S}_l^{(i+1)}$ ,  $\zeta_{j,k} = \zeta_{j,k}^{(i+1)}$  and obtain  $\eta^{(i+1)}$ ,  $t_p^{(i+1)}$ ,  $\xi_l^{(i+1)}$ ,  $\zeta_{j,k}^{(i+1)}$
  - 5:   Set  $i = i + 1$
  - 6: **until**  $\frac{|\bar{f}^{(i)} - \bar{f}^{(i-1)}|}{\bar{f}^{(i)}} \leq \delta$
- 

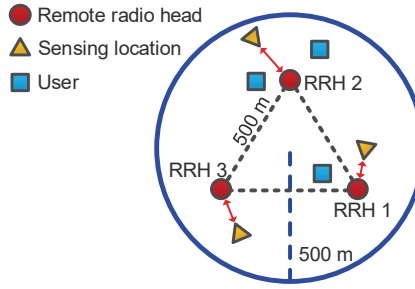


Fig. 2. Simulation setup for a distributed antenna multiuser ISAC system comprising  $J = 3$  RRHs,  $K = 3$  users, and  $L = 3$  sensing locations. The red double arrows indicate the pre-determined RRH-target pairs.

The three RRHs form an equilateral triangle with a side length of 500 m while the CP is located at the centroid of the triangle.  $K = 3$  users and  $L = 3$  sensing locations are uniformly and randomly distributed in a disc with a radius of 500 m centered at the location of the CP. The path loss exponents for the user channels and the channel between the RRHs and sensing locations are set to 3 and 2, respectively. The path loss at the reference distance of 1 m is set to 40 dB. We model the small-scale fading coefficients of the user channels as independent and identically distributed Rayleigh random variables. Each target location is assumed to be sensed by the nearest RRH employing a highly-directional beam. The angular domain is equally divided into  $I = 360$  directions to generate a set of  $\{P_l(\theta_i)\}_{i=1}^I$  based on the pre-determined RRH-target pairs. To facilitate the presentation, we define the normalized beam pattern mismatch tolerance error  $\bar{\epsilon}_l = \frac{\epsilon_l}{\sum_{i=1}^I P_l(\theta_i)}$  and set  $\bar{\epsilon}_l = 0.1$ . The parameters adopted in the simulations are summarized in Table I. For comparison, we also consider two baseline schemes. For baseline scheme 1, we consider an ISAC system with co-located transmit antennas, where a conventional

TABLE I  
SYSTEM SIMULATION PARAMETERS.

$\sigma_{U_k}^2$	Noise power at user $k$	$-104$ dBm
$T$	ISAC frame length	1 ms
$P_{T_j}^{\max}$	Maximum transmit power at each RRH	46.5 dBm [14]
$\bar{R}_{\text{req}_k}$	Required achievable rate of users	2 bits/s/Hz
$P_{\text{req}_l}$	Minimum required echo power	$-90$ dBm
$P_{\text{tol}_l}$	Maximum interference tolerance	$-100$ dBm
$C_F^{\max}$	Maximum fronthaul link capacity	5.5 bits/s/Hz
$N_b$	Number of bits for quantizing echoes	4
$M$	Number of rounds in sensing phase	100
$\Delta R$	Sensing resolution	10 m [4]
$W_F$	Fronthaul link bandwidth	10 MHz [15]
$t_{\min}$	Minimum pulse width	$0.1 \mu\text{s}$ [4]
$\psi_l$	Beamwidth of the ideal beam pattern	$\frac{\pi}{6}$ [4]
$\delta$	Convergence tolerance	$10^{-3}$
$\mu$	Penalty factor	$10^3$

BS with  $N_T J$  antennas and a power budget  $\sum_{j \in \mathcal{J}} P_{T_j}^{\max}$  is located at the center of the cell. In this case, there is no need for fronthaul links and a multi-beam pattern is designed to concurrently sense all target locations. The total energy consumption of the considered system is minimized subject to constraints C1-C7 and C10-C12 of (11) by employing the proposed algorithm. For baseline scheme 2, we equally allocate the time to communication and sensing and solve (11) for  $\eta = 0.5$ . The performance of the two baseline schemes will be shown in Fig. 5. We first study the performance of the proposed scheme by focusing on the scenario illustrated in Fig. 2. In Fig. 3, we show the time and energy used for communication and sensing for the proposed scheme with an ISAC frame duration of  $T = 1$  ms. We observe that most of the time (roughly 90%) is assigned to the communication phase as this is favorable to satisfy the achievable rate requirement of the users in a power-efficient manner. On the other hand, although the time allocated to target sensing is much less than that for information transmission, the RRHs in the sensing phase consume more energy compared to the communication phase. This is because in the sensing phase, a comparatively high power is needed to combat the severe round-trip path loss such that the received power of the echoes at the RRHs exceeds the noise floor for reliable detection. Moreover, in Fig. 4, we show the fronthaul data rate of each RRH and the sum data

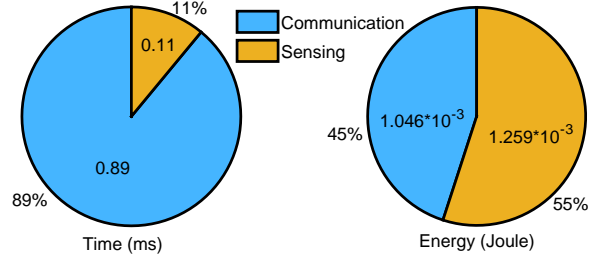


Fig. 3. Illustration of the time and energy consumed for communication and sensing for an ISAC frame duration of  $T = 1$  ms.

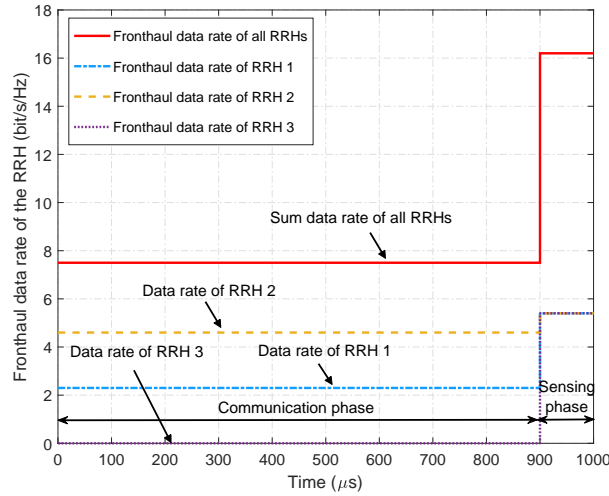


Fig. 4. Illustration of the fronthaul data rate of each RRH and the sum data rate of all fronthaul links during the communication and sensing phases of the proposed scheme.

rate of all fronthaul links. We observe that compared to the communication phase, there is more data traffic between the RRHs and the CP in the sensing phase. This is because to acquire the sensing information of the target location in a power-efficient manner, the minimum sensing range has to be short to save power while the maximum sensing range should be larger than the distance of each RRH-target pair, leading to a large amount of quantized sensing data, cf. (6). Furthermore, we also observe that during the communication phase, RRH 2 of the proposed scheme serves two users in its vicinity while RRH 3 is not used for information transmission as this is beneficial to improve power efficiency. In contrast, during the sensing phase, due to the pre-determined RRH-target pairs, each RRH senses a dedicated location and exchanges a similar amount of sensing data with the CP via the respective fronthaul link.

Fig. 5 shows the average total energy consumption during an ISAC frame (Joule) versus the



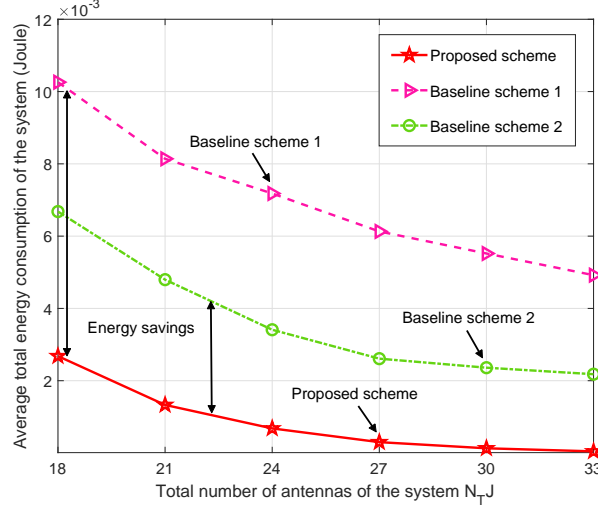


Fig. 5. Average total energy consumption during an ISAC frame (dBm) versus the total number of transmit antennas in the system,  $N_{TJ}$ , for different schemes.

total number of transmit antennas in the system for different schemes. As expected, for the proposed scheme and the two baseline schemes, the average total energy consumption during an ISAC frame decreases with  $N_{TJ}$ . In fact, by employing a larger set of antenna elements, the RRHs can exploit additional degrees-of-freedom (DoFs) to make the information beamforming power-efficient and to accurately synthesize the required energy-focused beam patterns, resulting in power savings. Moreover, compared to the proposed scheme, the two baseline schemes cause a significantly higher total energy consumption. This confirms the effectiveness of joint time, beamforming, and sensing signal optimization for the proposed DAN-based ISAC system. In particular, the co-located antenna architecture employed in baseline scheme 1 does not offer spatial macro-diversity to combat the path loss of the information and sensing signals. As for baseline scheme 2, although the RRHs can enjoy the performance gain introduced by the distributed antenna architecture, it is limited by the fixed duration of the communication and sensing phases.

## VI. CONCLUSIONS

In this paper, we studied the resource allocation algorithm design for DAN-based ISAC systems. In particular, to mitigate the mutual interference between sensing and communication, we proposed to perform sensing and communication in two different phases. Taking into account the limited capacity of the fronthaul links and the QoS requirements of both sensing and

communication, we minimized the total energy consumption of all RRHs over a given time horizon by jointly optimizing the durations of both phases, information beamforming, and sensing signal. An computationally-efficient AO-based algorithm was developed for tackling the resulting non-convex optimization problem which allowed us to obtain a suboptimal solution. Simulation results showed that the proposed scheme can achieve significant energy savings compared to two baseline schemes. Moreover, our results revealed that compared to information transmission, target sensing in general requires a higher transmit power to combat the round-trip path loss and is also more energy-hungry. Besides, our results revealed that compared to a conventional network with co-located antennas, the proposed DAN is a more promising architecture to facilitate future green ISAC systems.

## REFERENCES

- [1] A. Liu *et al.*, “A survey on fundamental limits of integrated sensing and communication,” *IEEE Commun. Surv. Tuts.*, vol. 24, no. 2, pp. 994–1034, Feb. 2022.
- [2] F. Liu, C. Masouros, A. Li, H. Sun, and L. Hanzo, “MU-MIMO communications with MIMO radar: From co-existence to joint transmission,” *IEEE Trans. Wireless Commun.*, vol. 17, no. 4, pp. 2755–2770, Apr. 2018.
- [3] Z. Ren, L. Qiu, and J. Xu, “Optimal transmit beamforming for secrecy integrated sensing and communication,” in *Proc. IEEE Intern. Conf. Commun. (ICC)*, Seoul, Korea, May 2022, pp. 5555–5560.
- [4] M. I. Skolnik, *Radar Handbook*. McGraw-Hill Education, 2008.
- [5] R. Irmer *et al.*, “Coordinated multipoint: Concepts, performance, and field trial results,” *IEEE Commun. Mag.*, vol. 49, no. 2, pp. 102–111, Feb. 2011.
- [6] D. W. K. Ng and R. Schober, “Secure and green SWIPT in distributed antenna networks with limited backhaul capacity,” *IEEE Trans. Wireless Commun.*, vol. 14, no. 9, pp. 5082–5097, Sept. 2015.
- [7] B. Tang and J. Li, “Spectrally constrained MIMO radar waveform design based on mutual information,” *IEEE Trans. Signal Process.*, vol. 67, no. 3, pp. 821–834, Feb. 2019.
- [8] F. Liu *et al.*, “Integrated sensing and communications: Towards dual-functional wireless networks for 6G and beyond,” *IEEE J. Sel. Areas Commun.*, vol. 40, no. 6, pp. 1728–1767, Jun. 2022.
- [9] J. Lu, T. Tian, Y. Tang, and B. Tang, “Performance analysis of data transmission for joint radar and communication systems,” *Math. Probl. Eng.*, vol. 2021, pp. 1–14, Mar. 2021.
- [10] D. Xu, X. Yu, D. W. K. Ng, A. Schmeink, and R. Schober, “Robust and secure resource allocation for ISAC systems: A novel optimization framework for variable-length snapshots,” *accepted to IEEE Trans. Commun.*, 2022.
- [11] J. Nocedal and S. Wright, *Numerical Optimization*. Springer, 1999.
- [12] X. Yu, D. Xu, D. W. K. Ng, and R. Schober, “IRS-assisted green communication systems: Provable convergence and robust optimization,” *IEEE Trans. Commun.*, vol. 69, no. 9, pp. 6313–6329, Sept. 2021.
- [13] J. C. Bezdek *et al.*, “Some notes on alternating optimization,” in *AFSS Int. Conf. Fuzzy Systems*. Springer, 2002, pp. 288–300.
- [14] Third Generation Partnership Project (3GPP), “Radio frequency system scenarios, version 13.0.0,” *3GPP TR 36.942 Release 13*, Jan. 2016.
- [15] K. M. S. Huq and J. Rodriguez, *Backhauling/Fronthauling for Future Wireless Systems*. John Wiley & Sons, 2016.